SCIENTIFIC REPORTS

OPEN

SUBJECT AREAS:
TERAHERTZ OPTICS
METAMATERIALS
NANOPHOTONICS AND PLASMONICS

Received
13 March 2014

Accepted
16 May 2014

Published
9 June 2014

Correspondence and requests for materials should be addressed to H.C. (hychoi@yonsei.ac.kr) or H.L. (hojinl@ssu.ac.kr)

* These authors contributed equally to this work.

Anisotropy Modeling of Terahertz Metamaterials: Polarization Dependent Resonance Manipulation by Meta-Atom Cluster

Hyunseung Jung[1]*, Chihun In[2]*, Hyunyong Choi[2] & Hojin Lee[1]

[1]School of Electronic Engineering, Soongsil University, Seoul 156-743, Korea, [2]School of Electrical and Electronic Engineering, Yonsei University, Seoul 120-749, Korea.

Recently metamaterials have inspired worldwide researches due to their exotic properties in transmitting, reflecting, absorbing or refracting specific electromagnetic waves. Most metamaterials are known to have anisotropic properties, but existing anisotropy models are applicable only to a single meta-atom and its properties. Here we propose an anisotropy model for asymmetrical meta-atom clusters and their polarization dependency. The proposed anisotropic meta-atom clusters show a unique resonance property in which their frequencies can be altered for parallel polarization, but fixed to a single resonance frequency for perpendicular polarization. The proposed anisotropic metamaterials are expected to pave the way for novel optical systems.

Over the last several years, metamaterials have attracted considerable attention for terahertz and optical applications, including unnaturally high refractive index[1] components, perfect absorbers[2–4], frequency tunable filters[5,6], and ultrafast switching devices[7]. The electromagnetic properties of metamaterials originate from the geometrical arrangement of the periodic unit cell called the meta-atom. By controlling the size[8], pitch[9–12], or shape[13] of the meta-atom on a single substrate, researchers have demonstrated metamaterials with exotic properties that do not exist in nature, such as negative refractive index[14], polarization conversion of an incident wave[15,16], and electric field enhancement[17]. In particular, the frequency selectivity of meta-atoms is one of the most important characteristics in designing metamaterials for terahertz applications; significant progress has been made in engineering resonance tendencies by manipulating the gap size or position of the entire structure[18,19], coupling effects between adjacent meta-atoms[12,20–23] such as Fano resonance[24–26], lattice modes of the metamaterial array[27,28], and dielectric effects of metamaterial substrates[29,30].

With respect to the meta-atom structure, unlike the structures of polarization independent metamaterials, such as the cross and ring-shaped structures[31–33], Split-ring resonators (SRRs), cut-wires (CWs)[34], or their complementary structures[35] are the most well-known metamaterial structures that exhibit anisotropic properties depending on the polarization property of the incident waves. Particularly, in the optical and terahertz regimes, planar SRR structures have a fundamental LC resonance, as well as a half wave resonance, (or plasmonic oscillation) along the side length of the SRR unit cell[8,36]. However, Rockstuhl et al.[18] were the first to conclude that the gap size variation of SRR structures could results in the resonance frequency change for perpendicular polarization in comparison to the half wave frequency of the side length of the SRRs. Since then, the unified interpretation of the anisotropic resonance mechanism for SRRs for different orders of standing waves (or plasmonic eigenmodes) has been suggested and widely utilized[13,27,37,38].

Although the anisotropic interpretation for incident polarization can explain the resonances in conventional SRR structures, it is difficult to apply this model to other, more complicated meta-atom structures. Consequently, the existing anisotropy models apply only to the SRR-like structures and their properties. Therefore, in order to understand the unique resonance mechanisms of complicated anisotropic meta-atom structures such as meta-atom clusters, a comprehensive model that can explain each of the resonance properties of anisotropic meta-atoms needs to be built.

In this paper, we propose an anisotropy model for anisotropic meta-atom clusters to elucidate their resonance mechanism depending on the polarization property of the incident waves. Using the proposed anisotropy model,

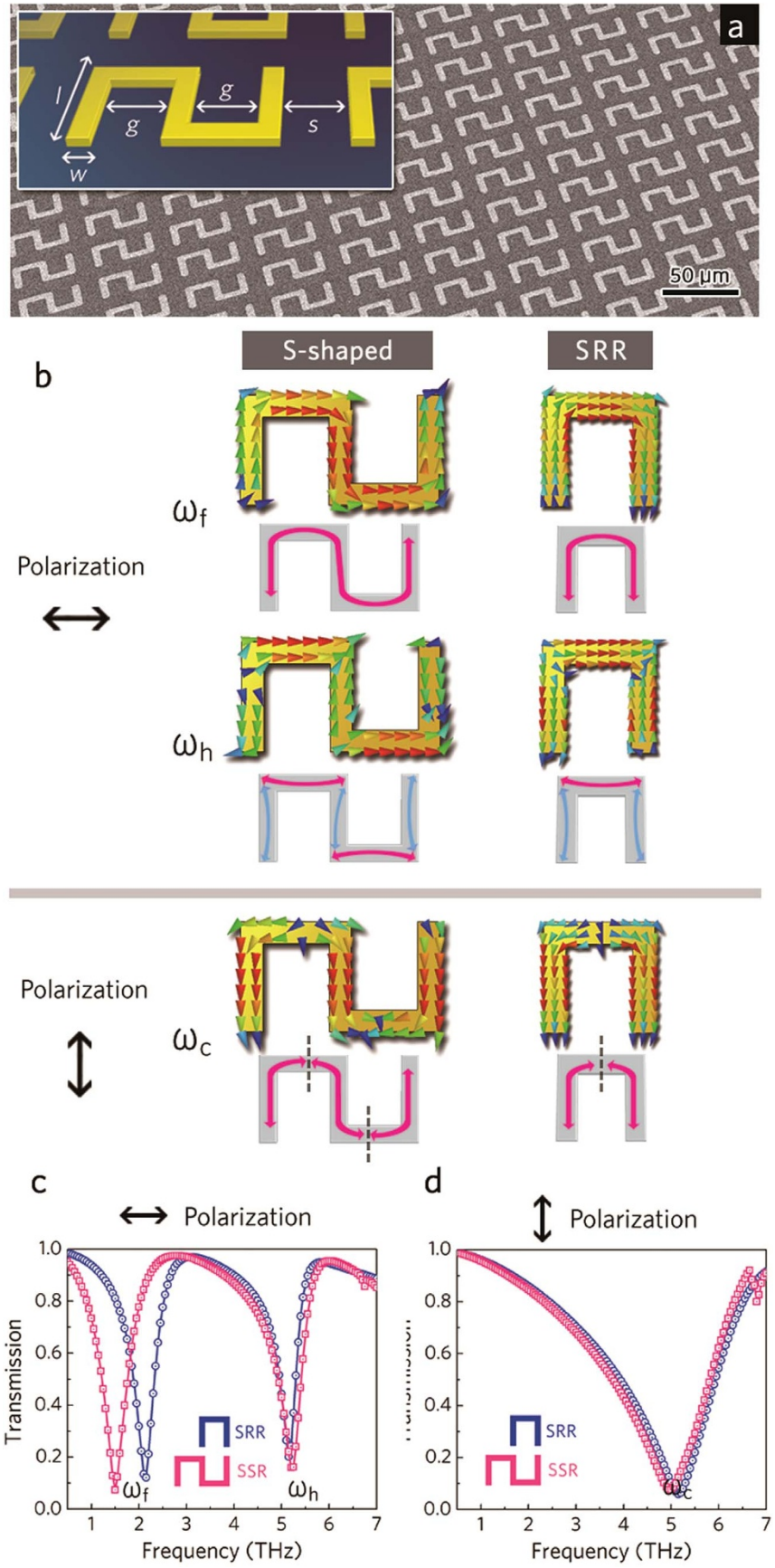

Figure 1 | S-shaped resonator (SSR) array. (a) Schematic and SEM image of the fabricated SSR metamaterial array. The unit cell has dimensions of $w = 4$ μm, $l = 20$ μm, and $g = s = 12$ μm. (b) Simulated surface current distributions of the SSR and SRR unit cells at ω_f, ω_h and ω_c, respectively. The charge collision regions are indicated by the dashed line. The simulated transmission spectra of the SSR and SRR array: (c) for parallel polarization and (d) for perpendicular polarization.

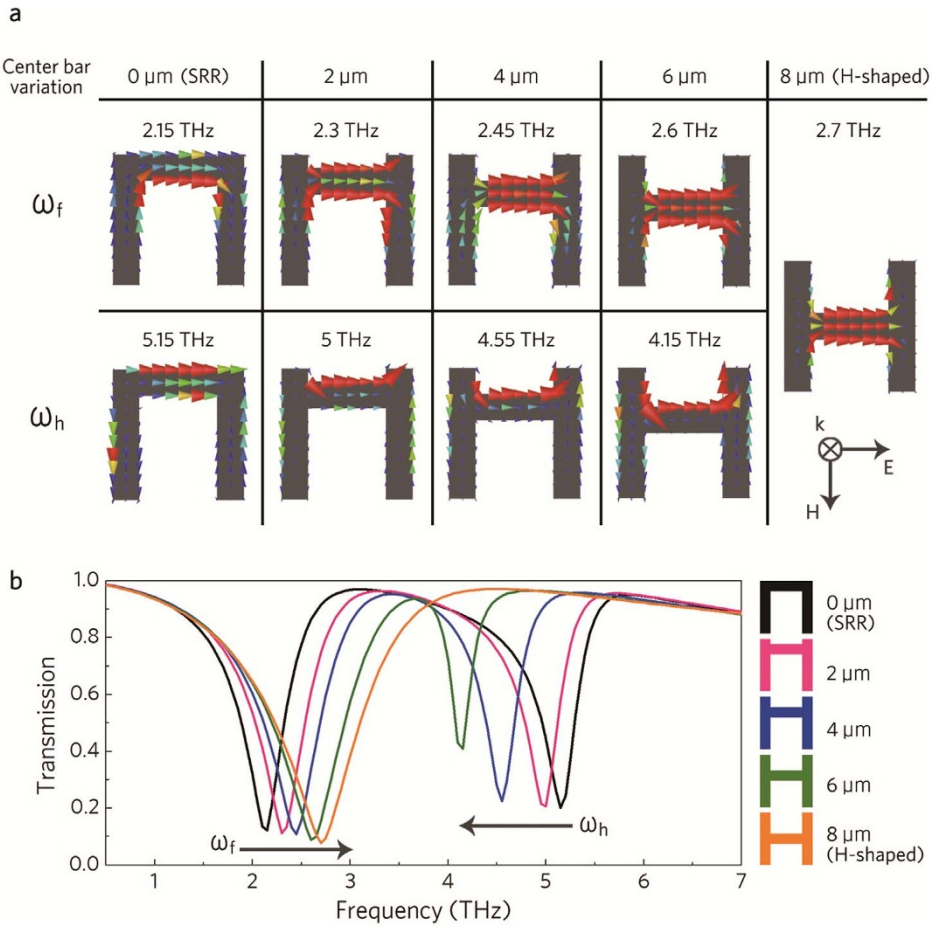

Figure 2 | The induced current distributions in various meta-atoms. Simulated (a) surface current distributions and (b) transmission spectra of various metamaterials from the conventional SRR to the H-shaped meta-atoms by shifting the center bar position by 2 μm. The 20 by 20-μm unit cell has a 4-μm line width. The incident electric field is polarized parallel to the gap of the unit cells. ω_f and ω_h represent the resonance frequencies on the inner and outer sides of the induced unit cells, respectively.

we confirm that the anisotropic meta-atom clusters we specifically designed can alter their resonance frequency under parallel polarization but fix their fundamental resonance frequency at a single frequency under perpendicular polarization, regardless of structural variations.

Results

Analysis of meta-atom strutures. First, we fabricated the S-shaped resonators (SSRs) array having a negative refractive index[39], and compared its resonance properties with the conventional SRR array. As shown in Figure 1a, the unit cell of the SSR structure consists of a pair of SRR structures, and it has a width (w) of 4 μm and length (l) of 20 μm with the gap (g) and space (s) both set to 12 μm. To analyze the actual metamaterial properties within the substrate, a 6-μm-thick polyimide substrate with assumed permittivity of 2.6 was considered for simulation. Figure 1b shows the surface current distributions of the SSR and SRR unit cells for each resonance frequency. In the SRR structure, resonances can be estimated by the different orders of standing waves and have odd symmetry for parallel polarization, whereas they have even symmetry for perpendicular polarization[13,37,38]. However, in the SSR structure as shown in Figure 1b, the resonances for the perpendicular polarization do not have even symmetry due to the structural difference. In addition, the higher order resonance (ω_h) for parallel polarization starts directly from the fifth order, skipping the third order resonance in the SRR structure. These results confirm that the resonance mechanism based on the odd and the even symmetry is valid only for the conventional SRR structure, but cannot be applied to SRR meta-atom clusters including the SSR structure.

Since the SRR and SSR unit cells act like two and three separate CW unit cells, respectively, for perpendicular polarization, we can assume that the pseudo-CW resonance frequency ω_c originates from the number of excited metal lines that are parallel to the polarization. Because all the charges in each metal line that is parallel to the incident E-field are excited concurrently for normal incidence, these moving charges should have the same direction and phase. Hence, as indicated by dashed line in Figure 1b, equally excited charges inevitably collide with each other at the connecting bridges of each SRR and SSR unit cells, preventing current flow by the Coulomb repulsive force. Consequently, the standing waves formed by the charge density in SRR and SSR unit cells have three and four nodes due to their one- and two-charge collision regions, respectively. As a result, as shown in Figures 1c and d, compared to a single SRR structure, the SSR structure has ω_c fixed near 5 THz with little variation of 2.9% (0.15 THz equivalently), while the fundamental frequency ω_f is remarkably red-shifted from 2.12 to 1.5 THz since the SSR unit cell does not have any charge collision for parallel polarization. The alteration ratio of ω_f is approximately 29.2%. The subtle difference of the ω_c between SRR and SSR is attributed to the difference in the actual wavelength, as shown by the red arrows in Figure 1b.

Although the variations of the resonance frequencies ω_f and ω_c can be explained by the direction of excited metal lines and their resulting charge collisions, the higher order resonance frequency ω_h for all meta-atoms cannot be explained either by a third order res-

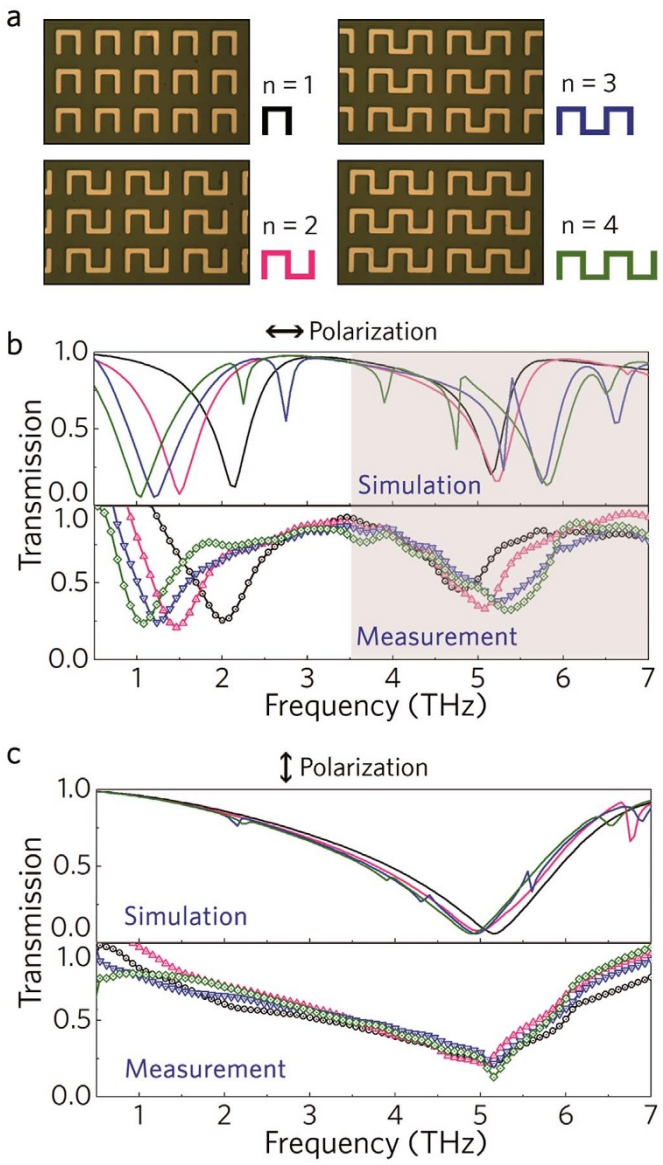

Figure 3 | Experimental results of combined SRR metamaterial array. (a) Optical microscopy images of the fabricated SSR metamaterials with different numbers (n) of combined SRR unit cells. Measured and simulated transmission spectra of the SSR metamaterials (b) for parallel polarization and (c) for perpendicular polarization. The higher order frequency components are considered as spectral noise shown as shaded areas in each figure.

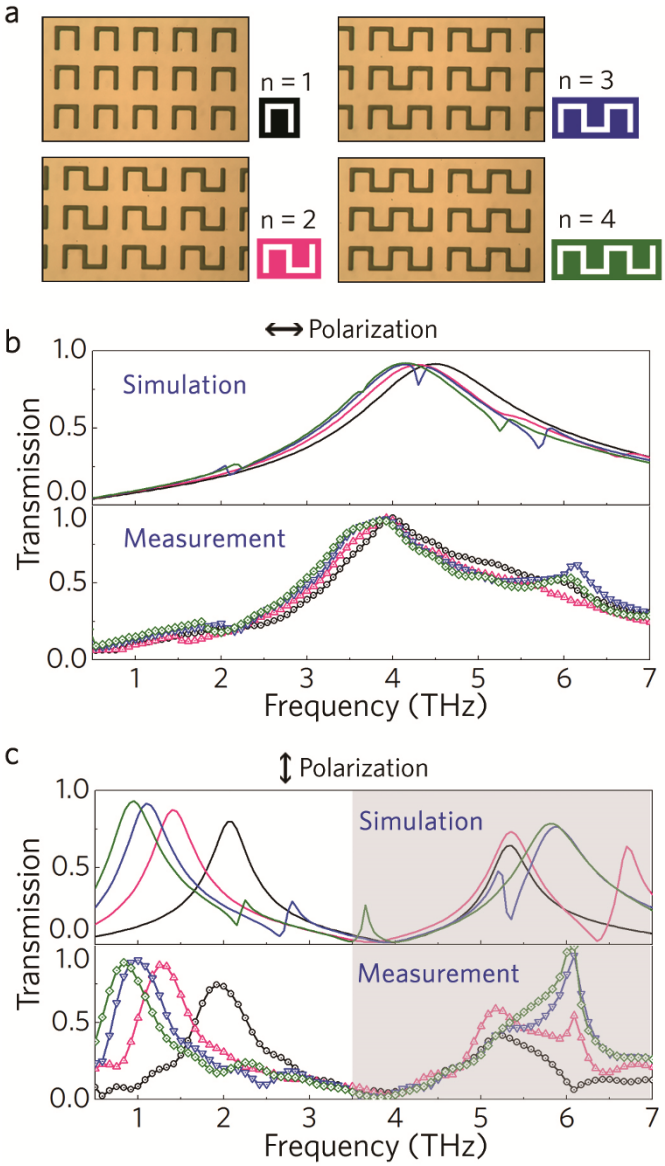

Figure 4 | Experimental results of combined complementary SRR metamaterial array. (a) Optical microscopy images of the fabricated complementary SSR metamaterials with different numbers (n) of combined complementary SRR unit cells. Measured and simulated transmission spectra of the complementary SSR metamaterials (b) for parallel polarization and (c) for perpendicular polarization. The higher order frequency components are considered as spectral noise shown as shaded areas in each figure.

onance or by the excited charge collision, as discussed above. In order to investigate the origin of the higher resonances for the parallel polarization in the SSR structure, we simulated the surface current distributions on various meta-atom structures from those with the conventional SRR to those with the H-shaped[40] meta-atoms by shifting the center bar position by 2 μm, as shown in Figure 2. As shown in Figure 2a, the induced currents of all the meta-atoms were concentrated on the inner side of the structure at ω_f, but were concentrated on the opposite side at ω_h.

If ω_h originates from other higher order resonances, ω_h must be blue-shifted as much as ω_f is blue-shifted, because all the higher order frequencies depend on the wavelengths of their fundamental frequencies. However, in our meta-atom structures, as the center bar position in the SRR shifted toward the H-shape, as shown in Figure 2b, ω_h red-shifted as much as the increase in the opposite side current path of the meta-atom, while ω_f blue-shifted because the decrease of the inner side current path. Moreover, ω_h vanished for the H-shaped meta-atom when the current paths on both sides of H-shape became perfectly symmetrical to each other.

These results verify that the ω_h of the proposed meta-atoms originate from the structural asymmetry of each meta-atom for the corresponding polarization direction, rather than from just following their lower orders of standing waves. Therefore, apart from the conventional resonance models, we propose a novel anisotropy model an anisotropic meta-atom with an asymmetrical structure depending on the polarization direction of the incident waves.

Polarization dependent metamaterial design. In order to verify the anisotropic resonant responses further, the proposed SSR metamaterials were fabricated by using the conventional photolithography technique. Figures 3a shows the fabricated anisotropic

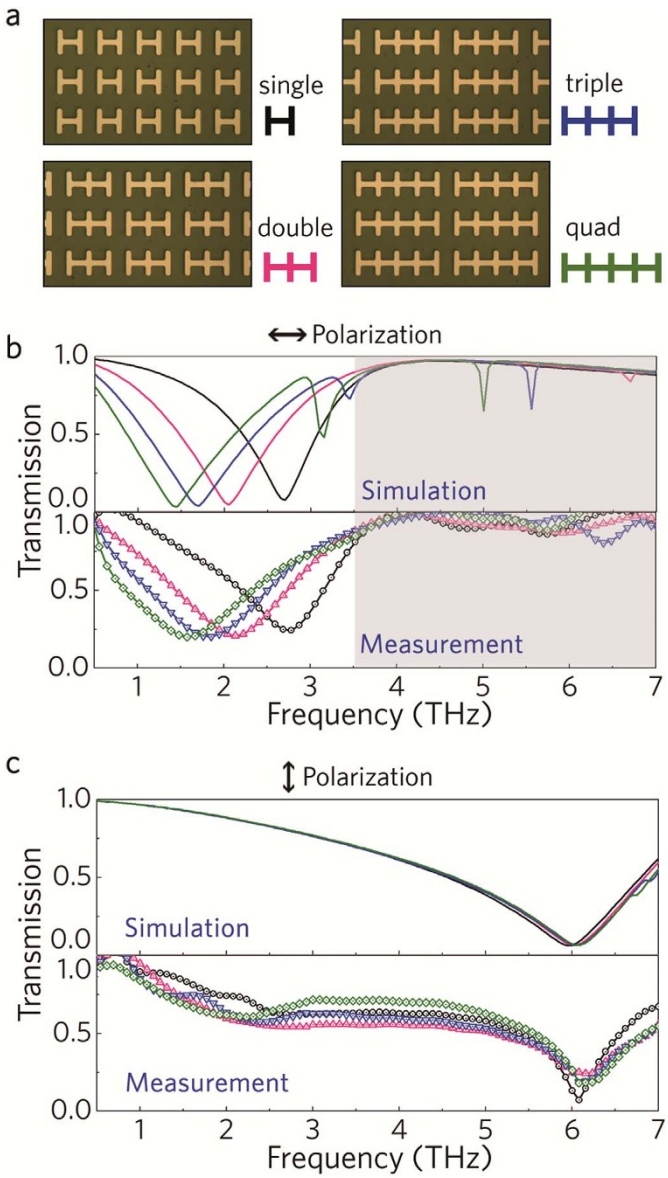

Figure 5 | Experimental results of H-shaped meta-atom cluster arrays. (a) Optical microscopy images of our fabricated H-shaped meta-atom clusters with different numbers (single, double, triple, and quad) of H-shaped unit cells. Measured and simulated transmission spectra of the proposed H-shaped metamaterials (b) for parallel polarization and (c) for perpendicular polarization.

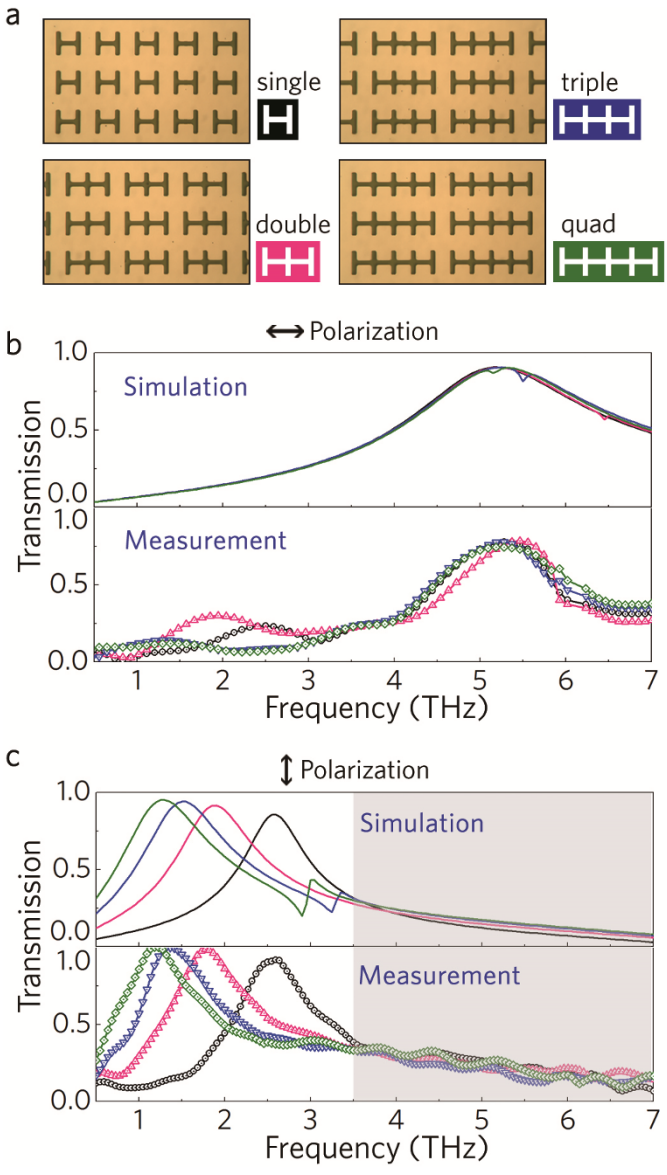

Figure 6 | Experimental results of complementary H-shaped meta-atom cluster arrays. (a) Optical microscopy images of our fabricated complementary H-shaped meta-atom clusters with different numbers (single, double, triple, and quad) of complementary H-shaped unit cells. Measured and simulated transmission spectra of the proposed complementary H-shaped metamaterials (b) for parallel polarization and (c) for perpendicular polarization.

SSR metamaterials. The detailed fabrication process is described in the Methods section. Figure 3b and c shows the measured transmission spectra for the SSR metamaterials in comparison with the simulated results. As shown in the figures, when the number of SRR cells increases from 1 to 4, the measured resonance frequency changes from 2.0, 1.45, 1.25, to 1.05 THz, respectively. On the other hand, for the perpendicular polarization, the resonance frequency of all SSR arrays stays near 5.1 THz with only small variations of less than 2%. Therefore, we confirm that the proposed anisotropic meta-atoms altered the resonance frequency for parallel polarization, and had a fixed resonance frequency for perpendicular polarization. Figure 3 also shows that the measured results well matched the simulation results. A slight discrepancy in the resonance between the simulated and the measured results is due to the variations in the fabrication process of the structure. Interestingly, the complementary structures showed exactly the same tendency with respect to the SSR metamaterials due to the Babinet principle, as shown in Figure 4[35,41,42]. Since the complementary structure has the opposite properties to the original structure, the proposed design methods can be utilized not only for the reflective, but also for the transmissive metamaterial array filters.

However, the higher resonance frequency components for parallel polarization still exist near the fixed resonance frequency (ω_c) for perpendicular polarization, working as spectral noise for utilizing the undisturbed ω_c. Therefore, to design the resonance frequencies of anisotropic metamaterials that can be altered for parallel polarization but completely fixed for perpendicular polarization (shown in Figure 5), we designed H-shaped meta-atom clusters that can maintain a symmetric current path for parallel polarization. The single H-shaped anisotropic meta-atom and its clusters (double, triple, and quad) act like identical CW unit cells, and the induced current also

has a completely symmetric current path for parallel polarization. Their characteristic resonance frequencies can be estimated by

$$\omega_f \approx \frac{c_{eff}}{2(nl+h)}, \quad (1)$$

$$\omega_c \approx \frac{c_{eff}}{2h}, \quad (2)$$

where c_{eff} is the speed of light divided by an effective refractive index, l and h are the center bar length and the side line height of the H-shaped meta-atom, respectively. n is the number of H-shaped meta-atoms in the proposed meta-atom clusters. These equations show that ω_c is independent of n and therefore constant, while the ω_f absolutely depends on n.

In order to verify the proposed equation for the H-shaped meta-atom clusters, we simulated and measured the transmission spectra, as shown in Figure 5b and c. The resonance frequencies of the single, double, triple, and quad meta-atom clusters for parallel polarization are 2.75, 2.15, 1.85, and 1.6 THz, respectively, while the resonance frequencies for perpendicular polarization are fixed at 6.1 THz for all structures. These results show that the results from the proposed equations well match with the measured resonances, and that the H-shaped anisotropic meta-atom and its clusters can alter the resonance frequency for parallel polarization, but fix the resonance frequency without any perturbation for perpendicular polarization, unlike the previous SSR metamaterial structures. Furthermore, as discussed above, the complementary H-shaped meta-atom clusters have similar resonance properties, as shown in Figure 6.

Discussion

We proposed a novel anisotropy model for the newly designed meta-atom clusters to predict their unique resonance properties depending on the polarization property of the incident waves. The experimental results showed that the proposed meta-atom clusters can alter their resonance by more than 1.1 THz for parallel polarization and can fix their resonance for perpendicular polarization. Moreover, based on the proposed anisotropy model, we showed that the meta-atom clusters can have only a fundamental frequency for any polarization in the desired frequency range, if their structures have a symmetric current path based on the excited metal line, like the H-shaped meta-atom clusters. Therefore, we expect that the proposed anisotropy model can provide an intuitive understanding of the resonance mechanism of anisotropic meta-atoms, for the development of novel optical systems, such as the polarization dependent multi-band terahertz system. Finally, our proposed anisotropy model can be applied to structures in fields ranging from microwave to optics by scaling the structures in electromagnetic-optical research.

Methods

Sample fabrication. The proposed anisotropic metamaterials were fabricated by a conventional photolithography process. First, 3 μm of polyimide was spin-coated on a silicon wafer and then baked at 90°C for 90 seconds and at 200°C for 120 seconds using a hot plate. After O_2 plasma treatment, 200-nm-thick gold with a 20-nm-thick chromium adhesion layer was deposited on the polyimide layer by an electron-beam evaporator and patterned by using the lift-off technique to form a meta-atom array. Then, 3 μm of polyimide was spin coated and baked as the passivation layer. Finally, the completed metamaterial film was peeled off from the wafer.

Terahertz measurements. For the terahertz (THz) time-domain spectroscopy measurements, 50 fs ultra-short pulses at 1.55 eV photon energy were produced by a Ti:sapphire regenerative amplifier (Coherent RegA 9050) operating at a 250 kHz repetition rate. A part of the amplifier output was used to generate THz pulses by optical rectification in a 320-μm-thick, (110)-oriented GaP crystal. The THz pulses with a 300-μm spot size were focused on the gold meta-atoms, which were deposited on a 2-mm-diameter polyimide (PI) substrate. The waveform of the transmitted THz pulses was measured by electro-optic sampling in an identical pair of GaP crystals. The transmittance of the meta-atoms in the THz frequency domain was obtained from the ratio of the transmitted THz field $E(\omega)$ through the samples and reference field $E_0(\omega)$ through the PI substrate. Our experimental setup provided THz bandwidths ranging from 0.5 THz to 7 THz, and whole apparatus was enclosed by dry air and an acrylic box to avoid THz absorption due to humidity.

1. Choi, M. *et al.* A terahertz metamaterial with unnaturally high refractive index. *Nature* **470**, 369–373 (2011).
2. Landy, N. I., Sajuyigbe, S., Mock, J. J., Smith, D. R. & Padilla, W. J. Perfect metamaterial absorber. *Phys. Rev. Lett.* **100**, 207402 (2008).
3. Tao, H. *et al.* A dual band terahertz metamaterial absorber. *J. Phys. D: Appl. Phys.* **43**, 225102 (2010).
4. Wen, Q.-Y., Zhang, H.-W., Xie, Y.-S., Yang, Q.-H. & Liu, Y.-L. Dual band terahertz metamaterial absorber: Design, fabrication, and characterization. *Appl. Phys. Lett.* **95**, 241111 (2009).
5. Ekmekci, E. at al. Frequency tunable terahertz metamaterials using broadside coupled split-ring resonators. *Phys. Rev. B* **83**, 193103 (2011).
6. Zhang, W. *et al.* Micromachined switchable metamaterial with dual resonance. *Appl. Phys. Lett.* **101**, 151902 (2012).
7. Lee, S. H. *et al.* Switching terahertz waves with gate-controlled active grapheme metamaterials. *Nat. Mater.* **11**, 936–941 (2012).
8. Linden, S. *et al.* Magnetic response of metamaterials at 100 terahertz. *Science* **306**, 1351–1353 (2004).
9. Sersic, I., Frimmer, M., Verhagen, E. & Koenderink, A. F. Electric and magnetic dipole coupling in near-infrared split-ring metamaterial arrays. *Phys. Rev. Lett.* **103**, 213902 (2009).
10. Liu, H. *et al.* Magnetic plasmon hybridization and optical activity at optical frequencies in metallic nanostructures. *Phys. Rev. B* **76**, 073101 (2007).
11. Liu, N., Liu, H., Zhu, S. & Giessen, H. Stereometamaterials. *Nat. Photon.* **3**, 157–162 (2009).
12. Liu, N. & Giessen, H. Coupling effects in optical metamaterials. *Angew. Chem. Int. Ed.* **49**, 9838–9852 (2009).
13. Rockstuhl, C. *et al.* On the reinterpretation of resonances in split-ring-resonators at normal incidence. *Opt. Express* **14**, 8827–8836 (2006).
14. Valentine, J. *et al.* Three-dimensional optical metamaterial with a negative refractive index. *Nature* **455**, 376–379 (2008).
15. Grady, N. K. *et al.* Terahertz metamaterials for linear polarization conversion and anomalous refraction. *Science* **340**, 1304–1307 (2013).
16. Cong, L. *et al.* A perfect metamaterial polarization rotator. *Appl. Phys. Lett.* **103**, 171107 (2013).
17. Seo, M. A. *et al.* Terahertz field enhancement by a metallic nano slit operating beyond the skin-depth limit. *Nat. Photon.* **3**, 152–156 (2009).
18. Rockstuhl, C. *et al.* Resonances of split-ring resonator metamaterials in the near infrared. *Appl. Phys. B* **84**, 219–227 (2006).
19. Singh, R., Al-Naib, I., Koch, M. & Zhang, W. Asymmetric planar terahertz metamaterials. *Opt. Express* **18**, 13044–13050 (2010).
20. Liu, N., Kaiser, S. & Giessen, H. Magnetoinductive and electroinductive coupling in plasmonic metamaterial molecules. *Adv. Mater.* **20**, 4521–4525 (2008).
21. Singh, R., Rockstuhl, C., Lederer, F. & Zhang, W. Coupling between a dark and a bright eigenmode in a terahertz metamaterial. *Phys. Rev. B* **79**, 085111 (2009).
22. Singh, R., Rockstuhl, C., Lederer, F. & Zhang, W. The impact of nearest neighbor interaction on the resonances in terahertz metamaterials. *Appl. Phys. Lett.* **94**, 021116 (2009).
23. Cao, W., Singh, R., Zhang, C., Han, J., Tonouchi, M. & Zhang, W. Plasmon-induced transparency in metamaterials: Active near field coupling between bright superconducting and dark metallic mode resonators. *Appl. Phys. Lett.* **103**, 101106 (2013).
24. Fedotov, V. A., Rose, M., Prosvirnin, S. L., Papasimakis, N. & Zheludev, N. I. Sharp trapped-mode resonances in planar metamaterials with a broken structural symmetry. *Phys. Rev. Lett.* **99**, 147401 (2007).
25. Singh, R., Al-Naib, I., Cao, W., Rockstuhl, C., Koch, M. & Zhang, W. The Fano resonance in symmetry broken terahertz metamaterials. IEEE Trans. *Tera. Sci. Tech.* **3**, 820–826 (2013).
26. Singh, R. *et al.* Observing metamaterial induced transparency in individual Fano resonators with broken symmetry. *Appl. Phys. Lett.* **99**, 201107 (2011).
27. Wallauer, J., Bitzer, A., Waselikowski, S. & Walther, M. Near-field signature of electromagnetic coupling in metamaterial arrays: a terahertz microscopy study. *Opt. Express* **19**, 17283–17292 (2011).
28. Singh, R., Rockstuhl, C. & Zhang, W. Strong influence of packing density in terahertz metamaterials. *Appl. Phys. Lett.* **97**, 241108 (2010).
29. Chiam, S.-Y., Singh, R., Zhang, W. & Bettiol, A. A. Controlling metamaterial resonances via dielectric and aspect ratio effects. *Appl. Phys. Lett.* **97**, 191906 (2010).
30. Shelton, D. J. *et al.* Effect of thin silicon dioxide layers on resonant frequency in infrared metamaterials. *Opt. Express* **18**, 1085–1090 (2010).
31. Landy, N. I. *et al.* Design, theory and measurement of a polarization-insensitive absorber for terahertz imaging. *Phys. Rev. B* **79**, 125104 (2009).
32. Kante, B. *et al.* Symmetry breaking and optical negative index of closed nanorings. *Nat. Commun.* **3**, 1180 (2012).
33. Lee, J.-W. *et al.* Relationship between the order of rotation symmetry in perforated apertures and terahertz transmission characteristics. *Opt. Eng.* **51**, 119002 (2012).
34. Liu, N. *et al.* Plasmon hybridization in stacked cut-wire metamaterials. *Adv. Mater.* **19**, 3628–3632 (2007).

35. Zentgraf, T. *et al.* Babinet's principle for optical frequency metamaterials and nanoantennas. *Phys. Rev. B* **76**, 033407 (2007).
36. Padilla, W. J., Taylor, A. J., Highstrete, C., Lee, M. & Averitt, R. D. Dynamical electric and magnetic metamaterial response at terahertz frequencies. *Phys. Rev. Lett.* **96**, 107401 (2006).
37. Bitzer, A., Ortner, A., Merbold, H., Feurer, T. & Walther, M. Terahertz near-field microscopy of complementary planar metamaterials: Babinet's principle. *Opt. Express* **19**, 2537–2545 (2011).
38. Cube, F. *et al.* Spatio-spectral characterization of photonic meta-atoms with electron energy-loss spectroscopy. *Opt. Mater. Express* **1**, 1009–1018 (2011).
39. Chen, H. *et al.* Left-handed materials composed of only S-shaped resonators. *Phys. Rev. E* **70**, 057605 (2004).
40. Li, J. *et al.* Mechanically tunable terahertz metamaterials. *Appl. Phys. Lett.* **102**, 121101 (2013).
41. Falcone, F. *et al.* Babinet principle applied to the design of metasurfaces and metamaterials. *Phys. Rev. Lett.* **93**, 197401 (2004).
42. Chen, H. T. *et al.* Complementary planar terahertz metamaterials. *Opt. Express* **15**, 1084–1095 (2007).

Acknowledgments

H.J. and H.L. were supported by Basic Research Laboratories (BRL) through NRF grant funded by the MEST (No.20110020262). C.I. and H.C. were supported by the National Research Foundation of Korea (NRF) grant funded by the Korea government (MSIP) (NRF-2011-0013255).

Author contributions

H.J. designed the anisotropic metamaterials and fabricated the samples. C.I. conducted terahertz measurements. H.L. and H.C. guided the research. H.J., C.I., H.C. and H.L. prepared the manuscript. All authors contributed to data analysis and discussions.

Additional information

Competing financial interests: The authors declare no competing financial interests.

How to cite this article: Jung, H., In, C., Choi, H. & Lee, H. Anisotropy Modeling of Terahertz Metamaterials: Polarization Dependent Resonance Manipulation by Meta-Atom Cluster. *Sci. Rep.* **4**, 5217; DOI:10.1038/srep05217 (2014).

This work is licensed under a Creative Commons Attribution-NonCommercial-ShareAlike 3.0 Unported License. The images in this article are included in the article's Creative Commons license, unless indicated otherwise in the image credit; if the image is not included under the Creative Commons license, users will need to obtain permission from the license holder in order to reproduce the image. To view a copy of this license, visit http://creativecommons.org/licenses/by-nc-sa/3.0/